CHEMISTRY OF MATERIALS

ARTICLE

pubs.acs.org/cm

Formation of Large-Area Nitrogen-Doped Graphene Film Prepared from Simple Solution Casting of Edge-Selectively Functionalized Graphite and Its Electrocatalytic Activity

In-Yup Jeon,[†,§] Dingshan Yu,[‡,§] Seo-Yoon Bae,[†] Hyun-Jung Choi,[†] Dong Wook Chang,[†] Liming Dai,[†,‡] and Jong-Beom Baek*[,†]

[†]Ulsan National Institute of Science and Technology (UNIST), Interdisciplinary School of Green Energy/Institute of Advanced Materials & Devices, 100 Banyeon, Ulsan 689-798, South Korea

[‡]Department of Macromolecular Science and Engineering, Case Western Reserve University, 10900 Euclid Avenue, Cleveland, Ohio 44106, United States

Supporting Information

ABSTRACT: "Pristine" graphite is edge-selectively functionalized with 4-aminobenzoic acid by a "direct" Friedel−Crafts acylation reaction in a polyphosphoric acid/phosphorus pentoxide medium to produce 4-aminobenzoyl edge-functionalized graphite (EFG). The EFG is readily dispersible in *N*-methyl-2-pyrrolidone (NMP). Subsequent solution casting leads to the formation of large-area graphene film on a silicon wafer. The film shows sheet resistances of 60 and 200 Ω/sq, respectively, before and after heat treatment at 900 °C in an argon atmosphere. Upon the heat treatment, the EFG film becomes a N-doped graphene (N-graphene) film to display outstanding electrocatalytic activity for oxygen reduction reaction (ORR).

KEYWORDS: graphite, graphene, edge-functionalization, nitrogen-doped graphene, electrocatalytic activity

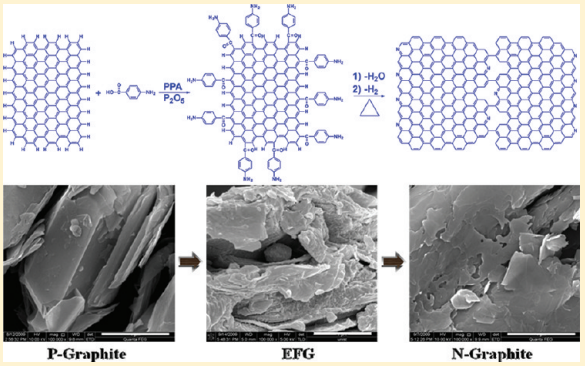

INTRODUCTION

The oxygen reduction reaction (ORR) at the cathode in a H_2/O_2 fuel cell has attracted particular attention, because the ORR is the most important process to control the cell performance.[1] Although platinum (Pt) has the highest electrocatalytic activity for ORR,[2] the major drawback of Pt-based cathode materials is that they tend to be inactivated by carbon monoxide (CO) poisoning and by agglomeration, in addition to its cost and scarcity.[3,4] Furthermore, a common pitfall for direct methanol fuel cells (DMFCs) has been the methanol crossover, which reduces cell performance.[5] A key issue in the development of fuel cells for practical applications is the search for lower cost and more-stable catalysts to replace expensive noble-metal-based electrodes. Recently, heterocyclic polymers,[6] N-doped carbon materials, such as vertically aligned N-doped carbon nanotubes (VA-NCNTs)[7] and N-doped graphene (N-graphene),[8] have attracted tremendous attention as long-term stable cathode materials for ORR, displaying even much improved catalytic activity and long-term stability over the commercially available Pt-based cathode (Vulcan XC-72R). These results strongly suggest potentials of fuel cells as one of the most promising sustainable energy resources. However, the scalability of VA-NCNT[7] and N-graphene[8,9] for large-quantity production is limited by chemical vapor deposition (CVD). Thus, a solvent-based preparation of N-graphene will be one of important advancements in commercialization of fuel cell technologies based on the metal-free N-doped carbon materials.[10−12]

We report the synthesis of scalable and high-quality N-graphene film via a simple solution processing and subsequent heat treatment of edge-selectively functionalized graphite (i.e., EFG) with 4-aminobenzoyl moieties. The desired EFG was prepared from the reaction between 4-aminobenzoic acid and "pristine" graphite (P-graphite) to afford 4-aminobenzoyl-functionalized graphite.[13] The EFG is readily dispersible in *N*-methyl-2-pyrrolidone (NMP). Solution casting and subsequent heat treatment can lead to the formation of large-area nitrogen-doped graphene (N-graphene) film. The 4-aminobenzoyl moieties (4-H_2N-Ph-CO−) at the edges of EFG can be the in-situ feedstock for carbon and nitrogen sources for "C-welding" and "N-doping" at the same time.

RESULTS AND DISCUSSION

Edge-functionalized graphite (i.e., EFG) was prepared from the reaction between 4-aminobenzoic acid and pristine graphite (P-graphite) to afford 4-aminobenzoyl-functionalized graphite (graphite-g-ABA, EFG) (see Scheme 1).[13] The reaction medium poly(phosphoric acid), PPA, used in this study is a viscous

Received: May 31, 2011
Revised: July 12, 2011
Published: August 02, 2011

dx.doi.org/10.1021/cm201542m | *Chem. Mater.* 2011, 23, 3987–3992

Scheme 1. Functionalization of Pristine Graphite (P-graphite) with 4-Aminobenzoic Acid To Produce Edge-Functionalized Graphite (EFG) with 4-Aminobenzoyl Groups and Subsequent Heat Treatment To Prepare Nitrogen-Doped Graphite (N-Graphite)

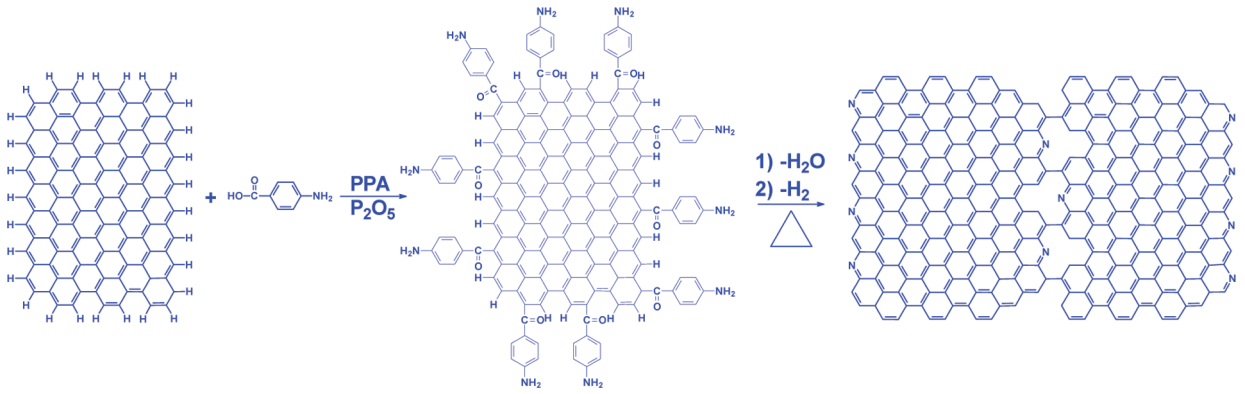

polymeric acid to provide strong shear while mechanically stirring, but not to damage carbon frameworks as a mild acid ($pK_a \approx 2.1$). It has many advantages for functionalization of carbon nanomaterials over the commonly used nitric acid ($pK_a = -1.5$)/sulfuric acid ($pK_a = -3.0$) mixture for the synthesis of graphite oxide (GO).[14,15] One of the salient features for the reaction conditions used in this study is that the reaction medium, PPA/P_2O_5, does not oxidize graphite but selectively functionalize the sp^2C-H defects at the edges of graphite (see Figure 1b).[13]

The resultant EFG can be readily dispersed in *N*-methyl-2-pyrrolidone (NMP). The EFG dispersion was then dip-coated on a glassy carbon (GC) electrode and heat-treated in situ at 900 °C for 3 h under argon atmosphere to afford the GC-supported "nitrogen-doped graphene" or N-graphene. During the heat treatment, the 4-aminobenzoyl moieties (4-H_2N-Ph-CO−) covalently attached to the edges of EFG were expected to be carbon and nitrogen sources for the in-situ "C-welding" and "N-doping" to produce a large-area N-graphene film coated on the GC electrode for the subsequent investigation of the ORR electrocatalytic activity.

Figure 1 shows the panoramic morphology changes in solid states from the P-graphite (Figure 1a) to EFG (Figure 1b) and heat-treated EFG (N-graphite, Figure 1c) upon the edge functionalization and subsequent heat treatment. As expected, TEM images from a holey carbon-coated grid dipped in the EFG dispersion in NMP show the presence of winkled graphene-like platelets (see Figures 2a−c). The corresponding TEM image obtained from the basal plain of EFG at a high magnification shows a highly crystalline graphene structure (see Figure 2d), implying that its basal plane has not been functionalized and/or damaged throughout the functionalization and workup processes. Although a dispersed EFG solution can give a mixture of single and few layer graphene platelets,[13] the TEM imaging focused on the edge of the EFG at a high magnification shows a single layer graphene sheet with a high crystalline interior plane and 4-aminobenzoyl moieties exclusively located on its edge (Figure 2e). The electron diffraction patterns clearly represent that the EFG consists of individual graphene and graphene-like platelets (insets, Figures 2d and 2e). For AFM analyses, a drop of the diluted EFG dispersion in NMP was placed on a silicon wafer and dried under reduced pressure. The AFM image and its corresponding topographic height

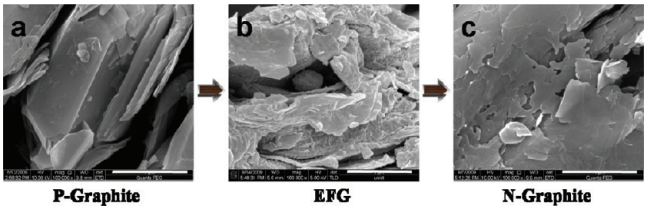

Figure 1. SEM images: (a) P-graphite, (b) EFG in solid state, and (c) N-graphite in solid state. Scale bars = 1 μm.

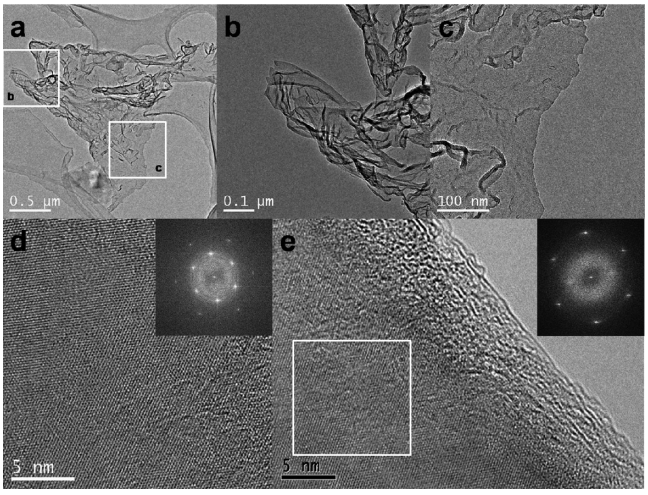

Figure 2. TEM images: (a−c) wrinkled EFG obtained from its dispersion in NMP; (d) TEM image obtained from EFG basal plane, showing the well-defined graphitic structure; and (e) TEM image focused on the EFG edge, showing the well-defined graphitic structure at interior part (see the white squared area) and the edge with functionalization. Insets are the selected-area electron diffraction (SAED) patterns from basal plane of the EFG, indicating a highly crystalline structure.

profiles also show the presence of the graphene-like structure with the layer height of ∼1 nm in Figure S1 in the Supporting Information. As expected, the height at the edge of the graphene sheet is higher than that of the inner layer, because the functionalization occurred exclusively at the edge of the graphite.

The aromatic 4-aminobenzoyl moieties on the EFG can thermally heal the damages on the carbon frame during the heat treatment, as indicated by the thermogravimetric analysis (TGA) results (see Figure S2 in the Supporting Information).[14,15] The TGA study also shows that the thermo-oxidative stability of EFG has greatly increased after 4-aminobenzoyl moieties were stripped off at 500−600 °C (see the sky blue oval region in Figure S2 in the Supporting Information). The result strongly implies that the heat treatment could convert the EFG to N-doped graphite (N-graphite) (Scheme 1). The 4-aminobenzoyl moieties act as the in situ feedstock for carbon and nitrogen sources for the thermal "C-welding" and "N-doping", respectively. The mechanism for thermal cyclization of EFG is proposed in two-step sequences (see Figure S3 in the Supporting Information).[16,17] The N-graphene could be produced in large quantities via a simple solution casting of EFG dispersion and subsequent heat treatment. The resultant large-area N-graphene film could be very useful as the electrocatalytic catalysts for ORR.[7,8]

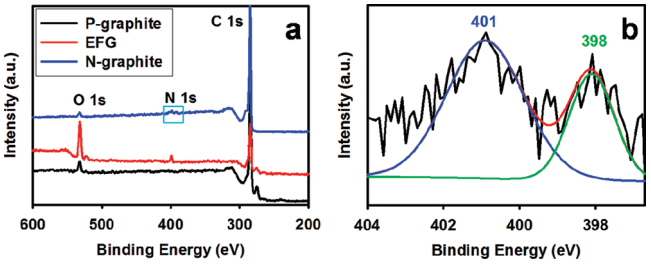

Figure 3. XPS spectra obtained from bulk samples: (a) full spectrum and (b) magnified spectrum in the N 1s region of N-graphite (sky blue square in panel a), showing peaks from pyridine-like and pyrrolic-like nitrogen at 398 and 401 eV, respectively.

Table 1. XPS Analysis Data for Samples

	Composition (%)		
sample	C	N	O
P-graphite	85.05	BDL[a]	14.92
EFG	74.81	6.65	18.54
N-graphite	95.16	1.73	1.78

[a] Below the detection limit.

Based on the TGA result, the bulk EFG was heat-treated at 900 °C under an argon atmosphere for 3 h. As shown in Figure 3a and summarized in Table 1, XPS measurements on the EFG revealed the expected composition of carbon, oxygen, and nitrogen. XPS analysis clearly shows the presence of nitrogen (ca. 1.73 at. %) after heat treatment. Curve fitting of the XPS N 1s reveals peaks at 398 and 401 eV (see Figure 3b), corresponding to pyridine-like and pyrrolic-like nitrogen, respectively.[18−20] Thereafter, we designate the N-graphite thus produced as "heat-treated EFG".

From Raman spectra obtained from bulk N-graphite shown in Figure S4 in the Supporting Information, the I_D/I_G intensity ratio of the bulk P-graphite and N-graphite were 0.06 and 0.14, respectively, implying that the defect ratio is increased slightly, because of the N-doping. The sheet resistance of the as-cast EFG film (Figure 4a) on a silicon wafer from a NMP solution was found to be 60 ± 5 Ω/sq, which is a value that is several orders of magnitude lower than that of an insulating graphene oxide (GO) film,[21] and even much lower than that of the chemically reduced graphene oxide (rGO) film.[22] However, the heat treatment increased the resistance up to 200 ± 28 Ω/sq for the heat-treated EFG film on a silicon wafer (Figure 4b), albeit still much lower than that of rGO. Relatively much lower sheet resistance, compared to that of rGO, should be originated from a highly graphitic structure (see Figure 2). The observed increase in resistance from EFG to N-graphene can be attributed to structural defects by C-welding at grain boundary and wrinkles induced by N-doping at the elevated temperature (see Figure 4b and Figure S5 in the Supporting Information).

To test the electrocatalytic activity, the EFG solution in NMP was dip-coated on a glassy carbon (GC) electrode and heat-treated at 900 °C for 3 h under an argon atmosphere to afford N-graphene/GC electrodes. For comparison, Figure 5a presents CV curves of the as-cast EFG on a GC electrode in 0.1 M aqueous KOH solution saturated with N_2 or O_2 with a scan rate of 0.01 V/s. Featureless voltammetric currents within the potential range of −1.0 V to 0.2 V were observed for EFG in N_2 saturated aqueous KOH solution (0.1 M), whereas the reduction of oxygen occurred at the potential of −0.15 V, when the electrolyte solution is saturated with O_2. In the case of N-graphene film on a GC electrode, the change in current density is profoundly higher than that in EFG, indicating high oxygen reduction activity (Figure 5b). Figure 5c shows rotating disk electrode (RDE) voltammograms of the EFG and N-graphene. Although the N-doping level may significantly influence the performance

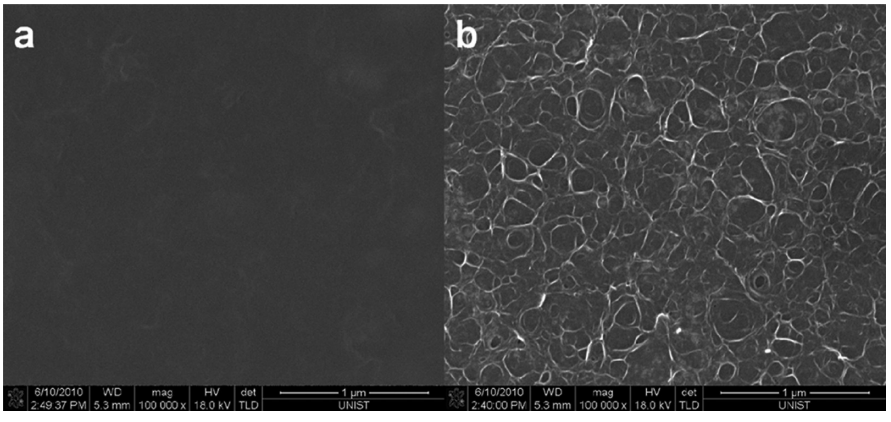

Figure 4. SEM images: (a) as-cast EFG film on silicon wafer by drop coating of EFG dispersed solution in NMP; (b) heat-treated EFG (N-graphene) film on silicon wafer at 900 °C under an argon atmosphere.

dx.doi.org/10.1021/cm201542m |*Chem. Mater.* 2011, 23, 3987–3992

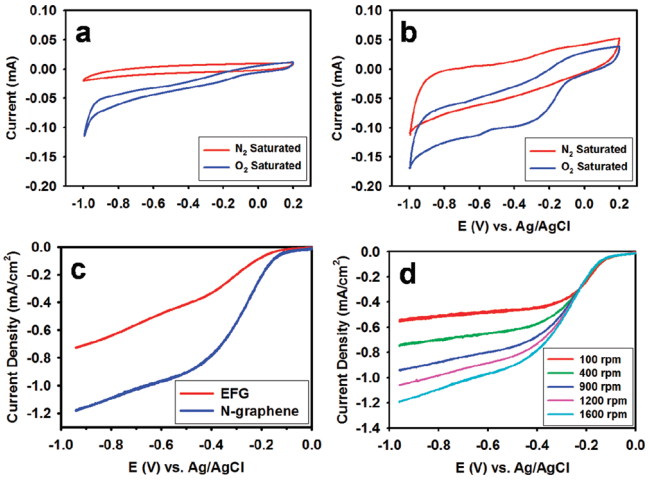

Figure 5. Cyclic voltammograms of sample film/glassy carbon (GC) electrodes in an O_2 saturated and an N_2 saturated 0.1 M aqueous KOH solution with a scan rate of 0.1 V/s: (a) EFG and (b) N-graphene. (c, d) Rotating disk electrode (RDE) voltammograms of sample film/GC electrodes in an O_2 saturated 0.1 M aqueous KOH solution with a scan rate of 0.01 V/s: (c) at a rotate rate of 1600 rpm; and (d) at different rotate rates of 100, 400, 900, 1200, and 1600 rpm of N-graphene film.

of ORR catalysis,[23−25] the oxygen reduction activity of the N-graphene is obviously more pronounced and similar to that of N-graphene prepared by CVD.[8] Although N-graphene (nitrogen content, ca. 1.7 at. %) from EFG has lower N-doping level than that (nitrogen content, ca. 4.0 at. %) from CVD,[8] similar catalytic activity can be attributed to wrinkles, which provide a larger surface area (see Figure 4b). Compared to commercially available platinum (Pt) on activated carbon (Pt/C, Vulcan XC-72R) supported by a GC electrode, the steady-state catalytic current density at the N-graphene electrode was found to be ~4 times higher than that of a Pt/C electrode over a large potential range.[8] In addition, the electrocatalytic activity of N-graphene is ~40 times higher than that of rGO (see Figure S6 in the Supporting Information).

To gain further insight into the role of N-graphene/GC electrode during the ORR process, the reaction kinetics by rotating-disk voltammetry was investigated (see Figure 5d and Figure S7 in the Supporting Information). The voltammetric profiles showed that the current density was increased by increasing the rotating rate. The onset potentials of EFG/GC and N-graphene/GC for ORR were approximately −0.15 and −0.13 V, respectively, which are close to that identified from CV measurements (Figure 5a and 5b). The corresponding Koutecky−Levich at various electrode potentials revealed parallel plots with a good linearity at different potentials (see Figure S8 in the Supporting Information), which are often taken as an indication of first-order reaction kinetics, with respect to the concentration of dissolved O_2.[26] The kinetic parameters can be analyzed on the basis of the Koutecky−Levich equation,[27] which was used to determine the transferred electrons number involved in oxygen reduction using graphene.[28,29] The equation is valid for a first-order process, with respect to the diffusion species, and the current density j is related to the rotation rate ω of the electrode, according to

$$\frac{1}{j} = \frac{1}{j_k} + \frac{1}{B\omega^{0.5}} \quad (1)$$

where j_k is the kinetic current and B is the Levich slope, which is given by

$$B = 0.2nF(D_{O_2})^{2/3}\nu^{-1/6}C_{O_2} \quad (2)$$

Here, n is the number of electrons transferred for the reduction of one O_2 molecule, F the Faraday constant (F = 96 485 C/mol), D_{O_2} the diffusion coefficient of O_2 ($D_{O_2} = 1.9 \times 10^{-5}$ cm^2 s^{-1}), ν the kinetic viscosity for KOH (ν = 0.01 cm^2 s^{-1}), and C_{O_2} the concentration of O_2 in the solution ($C_{O_2} = 1.2 \times 10^{-6}$ mol cm^{-3}). The constant 0.2 is adopted when the rotation speed is expressed in units of revolutions per minute (rpm). According to the above equation, the number of electron transferred (n) can be obtained from the slope of the Koutecky−Levich plots. The n values were calculated to be in the range of 3.2−3.5 (see Figure S8a and Table S1 in the Supporting Information). Similar to the value obtained from N-graphene prepared by CVD,[8] suggesting that the N-graphene leads to a four-electron transfer in oxygen reduction process, while EFG leads to a two-electron transfer (see Figure S8b in the Supporting Information).

We also investigated the electrochemical stability under ORR conditions for the N-graphene in O_2-saturated KOH for 3 days using a chronoamperometric method. The relative current−time (i−t) chronoamperometric response of the N-graphene/GC electrode exhibits a very slow attenuation. A high and steady relative current was still 87% under continuous ORR condition after 3 days. The result indicates that the catalytic sites of the N-graphene are very stable in the base medium. The test period is too short for commercial demands. However, it is already known that N-graphene prepared from CVD is stable up to 200 000 cycles,[8] endorsing that N-graphene in this study supposes to display similar performance. As can be seen from Figure 6b, the relative i−t chronoamperometric response of the N-graphene/GC electrode do not show any obvious change in an O_2 saturated 0.1 M aqueous KOH solution after adding 3 M methanol, which suggests that the corresponding effect of methanol crossover on the electrode is almost negligible.[30]

CONCLUSIONS

Edge-functionalized graphite (EFG) with aminobenzoyl moiety, which could be in-situ feedstock for "C-welding" and "N-doping" at the same time, was simply prepared via a one-pot reaction.[13] The EFG was well dispersible in NMP to produce graphene and graphene-like platelets. The procedure demonstrated in the present study is simple, but very efficient for a large-scale production of graphene platelets without introducing any oxygen-containing surface groups on the graphene basal plane. Thus, the large-area graphene film could be prepared from solution casting on silicon wafer and, thus, it showed low sheet resistance (as low as 60 Ω/sq). The N-graphene/glassy carbon (N-graphene/GC) electrode can also be simply formed by solution casting on the GC electrode and subsequent heat treatment. The resultant N-graphene/GC electrode showed similar ORR performance with N-graphene/GC electrode prepared from the CVD process. These results ensure scalable and high-quality production of N-graphene for cathode material in fuel cells[31] and metal-air batteries[32] in practice.

EXPERIMENTAL SECTION

Materials. All reagents and solvents were purchased from Aldrich Chemicals, Inc., and used as received, unless otherwise mentioned.

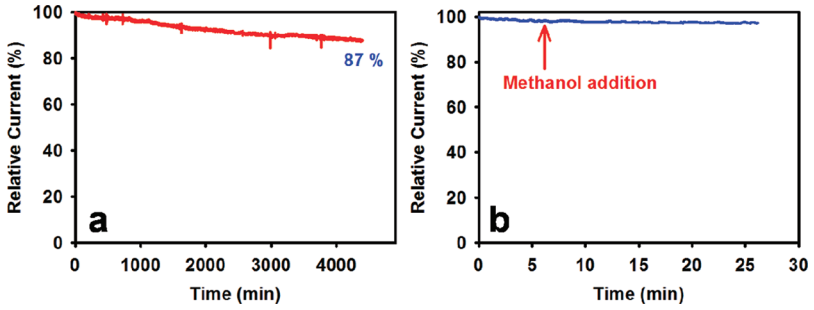

Figure 6. (a) Relative current−time ($i-t$) chronoamperometric response of the N-graphene/GC electrode at −0.3 V in an O_2 saturated 0.1 M aqueous KOH solution with a rotation rate of 1600 rpm for 3 days; (b) relative $i-t$ chronoamperometric response at the N-graphene/GC electrode at −0.3 V in an O_2 saturated 0.1 M aqueous KOH solution with the addition of 3 M methanol at ∼400 s, as indicated by the arrow. The *Y*-axis represents the percentage of current remaining with time, relative to the initial current.

4-Aminobenzoic acid as a reactive molecular wedge was purified by recrystallization from water. Graphite was obtained from Aldrich Chemicals, Inc., and was used as received. The commercial-grade platinum (Pt) on an activated carbon catalyst (Pt/C, C2−20, 20% HP Pt on Vulcan XC-72R, E-TEK Division, PE-MEAS Fuel Cell Technologies) was provided by BASF Fuel Cells.

Instrumentation. Infrared (Fourier transform infrared (FT-IR)) and Fourier transform (FT)-Raman spectra were recorded on a Fourier-transform spectrophotometer (Bruker, Model IFS-66/FRA106S). FT-Raman spectra were taken with 46-mW argon-ion laser (1064 nm) as the excitation source. Themogravimetric analysis (TGA) was conducted in air and argon atmospheres at a heating rate of 10 °C/min, using a TA Hi-Res TGA 2950 thermogravimetric analyzer. Field-emission scanning electron microscopy (FE-SEM) analysis was performed on LEO Model 1530FE and FEI Model NanoSem 200 systems, while field-emission transmission electron microscope (FE-TEM) images were taken on a FEI Tecnai G2 F30 S-Twin under an operating voltage of 200 kV. The samples for electron microscopy were prepared by dispersion in *N*-methyl-2-pyrrolidone (NMP). X-ray photoelectron spectroscopy (XPS) was performed on Thermo Fisher K-alpha (the detection limit is ca. 0.01). Elemental analysis (EA) was conducted using the Thermo Scientific Flash 2000 system. Atomic force microscopy (AFM) analysis was conducted with Veeco Multimode V.

Procedure for the Functionalization of Graphite with 4-Aminobenzoic Acid in Polyphosphoric Acid (PPA)/Phosphorus Pentoxide (P_2O_5). Graphite was functionalized with 4-aminobenzoic in a 250-mL resin flask equipped with a high-torque mechanical stirrer, a nitrogen inlet, and an outlet.[13] Into the flask, 4-aminobenzoic acid (0.5 g, 3.6 mmol), graphite mesh (0.5 g), PPA (83% P_2O_5 assay: 20.0 g), and P_2O_5 (5.0 g) were placed and stirred under dry nitrogen purge at 130 °C for 72 h. The initially black mixture became lighter and viscous as the functionalization onto graphite progressed. At the end of the reaction, the color of the mixture turned tanned brown, and water was added into the flask. The resultant tanned brown precipitate was collected by suction filtration, Soxhlet-extracted with water for three days, and then with methanol for three more days. Finally, the sample was dried over phosphorus pentoxide under reduced pressure (0.5 mmHg) at 100 °C for 72 h to give 0.74 g (79% yield) of tanned brown powder. Anal. Calcd. for $C_{26.70}H_6NO$: C, 89.90%; H, 1.70%; N, 3.93%; O, 4.48%. Found: C, 86.41%; H, 1.54%; N, 3.81%; O, 6.02%.

Electrochemical Study. Cyclic voltammetry (CV) measurements were performed using a computer-controlled potentiostat (CH Instruments, Model CHI 760 C) in a standard three-electrode cell. Samples/glassy carbon (GC) electrode was used as the working electrode, a platinum wire as the counter electrode, and an Ag/AgCl (3 M KCl filled) electrode as the reference electrode. Rotating disk electrode (RDE) experiments were carried out on a MSRX electrode rotator (Pine Instruments) and the CHI 760 C potentiostat. For all CV and RDE measurements, an aqueous solution of KOH (0.1 M) was used as the electrolyte. N_2 or O_2 was used to purge the solution to achieve oxygen-free or oxygen-saturated electrolyte solution.

The procedures of GC electrode pretreatment and modification are described as follows: prior to use, the working electrode was polished with alumina slurry to obtain a mirror-like surface and then washed with deionized (DI) water and allowed to dry. The EFG (1 mg) was dissolved in 1 mL solvent mixture of Nafion (5%) and EtOH/water (v/v = 1:9) by sonication. The EFG suspension (5 μL) was pipetted on the glassy carbon (GC) electrode surface, followed by drying at room temperature. Heat treatment of EFG/GC to N-graphene/GC was conducted in argon (200 SCCM) at 900 °C for 3 h.

■ ASSOCIATED CONTENT

Supporting Information. AFM image, TGA thermograms, annealing mechanism, Raman spectra, digital photo, Koutecky−Levich plots, and kinetic data. (PDF) This material is available free of charge via the Internet at http://pubs.acs.org.

■ AUTHOR INFORMATION

Corresponding Author

*E-mail: jbbaek@unist.ac.kr.

Author Contributions

§Authors contributed equally to this work.

■ ACKNOWLEDGMENT

This research was supported by WCU (World Class University), U.S.−Korea NBIT, and Basic Research Laboratory (BRL) programs through the National Research Foundation (NRF) of Korea funded by the Ministry of Education, Science and Technology (MEST), and U.S. Air Force Office of Scientific Research through Asian Office of Aerospace R&D (AFOSR-AOARD).

■ REFERENCES

(1) Sarah, C. B. *Platinum Met. Rev.* **2005**, *49*, 27.
(2) Mehta, V.; Cooper, J. *J. Power Sources* **2003**, *114*, 32.
(3) Blomen, L.; Mugerwa, M. In *Fuel Cell Systems*; Plenum Press: New York, 1993.
(4) Iwase, M.; Kawatsu, S. In *Proceedings of the 1st International Symposium on Proton Conducting Membrane Fuel Cells*, Vol. 1; 1995; p 12.

(5) Ren, X.; Zelenay, P.; Thomas, S.; Davey, J.; Gottesfeld, S. *J. Power Sources* **2000**, *86*, 111.
(6) Winther-Jensen, B.; Winther-Jensen, O.; Forsyth, M.; MacFarlane, D. R. *Science* **2008**, *321*, 671.
(7) Gong, L.; Du, F.; Xia, Z.; Durstock, M.; Dai, L. *Science* **2009**, *323*, 760.
(8) Qu, L.; Liu, Y.; Baek, J.-B.; Dai, L. *ACS Nano* **2010**, *4*, 1321.
(9) Wei, D.; Liu, Y.; Wang, Y.; Zhang, H.; Huang, L.; Yu, G. *Nano Lett.* **2009**, *9*, 1752.
(10) Panchakarla, L. S.; Subrahmanayam, K. S.; Saha, S. K.; Govindaraj, A.; Krishnamurthy, H. R.; Waghmare, U. V.; Rao, C. N. R. *Adv. Mater.* **2009**, *21*, 4726.
(11) Li, X.; Wang, H.; Robinson, J. T.; Sanchez, H.; Diankov, G.; Dai, H. *J. Am. Chem. Soc.* **2009**, *131*, 15939.
(12) Wang, X.; Li, X.; Zhang, L.; Yoon, Y.; Weber, P. K.; Wang, H.; Guo, J.; Dai, H. *Science* **2009**, *324*, 768.
(13) Choi, E.-K.; Jeon, I.-Y.; Bae, S. Y.; Lee, H.-J.; Shin, H. S.; Dai, L.; Baek, J.-B. *Chem. Commun.* **2010**, *46*, 6320.
(14) He, H.; Klinowski, J.; Forster, M.; Lerf, A. *Chem. Phys. Lett.* **1998**, *287*, 53.
(15) Lerf, A.; He, H.; Forster, M.; Klinowski, J. *J. Phys. Chem. B* **1998**, *102*, 4477.
(16) Horaguchi, T.; Oyanagi, T.; Creencia, E. C.; Tanemura, K.; Suzuki, T. *J. Heterocyclic Chem.* **2004**, *41*, 1.
(17) Higuchi, M.; Yamamoto, K. *Polym. Adv. Technol.* **2002**, *13*, 765.
(18) Nakajima, T.; Koh, M. *Carbon* **1997**, *35*, 203.
(19) Yatsimirskii, K.; Nemoskalenko, V.; Aleshin, V.; Bratushko, Y.; Moiseenko, E. *Chem. Phys. Lett.* **1977**, *52*, 481.
(20) Yang, Z.; Xia, Y.; Mokaya, R. *Chem. Mater.* **2005**, *17*, 4502.
(21) Park, S.; Ruoff, R. *Nat. Nanotechnol.* **2009**, *4*, 217.
(22) Gómez-Navarro, C.; Weitz, R. T.; Bittner, A. M.; Scolari, M.; Mews, A.; Burghard, M.; Kern, K. *Nano Lett.* **2007**, *7*, 3499.
(23) Lee, S. H.; Lee, D. H.; Lee, W. J.; Kim, S. O. *Adv. Funct. Mater.* **2011**, *21*, 1338.
(24) Lee, D. H.; Lee, W. J.; Kim, S. W. *Nano Lett.* **2009**, *9*, 1427.
(25) Lee, D. H.; Lee, W. J.; Kim, S. O.; Kim, Y.-H. *Phys. Rev. Lett.* **2011**, *106*, 175502.
(26) Bard, A. J.; Faulkner, L. R. *Electrochemical Methods: Fundamental and Applications*, 2nd Ed.; Wiley: New York, 2001; Chapter 9.
(27) Tammeveski, K.; Tenno, T.; Claret, J.; Ferrater, C. *Electrochim. Acta* **1997**, *42*, 893.
(28) Paulus, U. A.; Schmidt, T. J.; Gasteiger, H. A.; Behm, R. J. *J. Electroanal. Chem.* **2001**, *495*, 134.
(29) Lee, D. H.; Lee, W. J.; Lee, W. J.; Kim, S. O.; Kim, Y.-H. *Phys. Rev. Lett.* **2011**, *106*, 175502.
(30) Cui, H.-F.; Ye, J.-S.; Liu, X.; Zhang, W.-D.; Sheu, F.-S. *Nanotechnology* **2006**, *17*, 2334.
(31) Yu, D.; Nagelli, E.; Du, F.; Dai, L. *J. Phys. Chem. Lett.* **2010**, *1*, 2165.
(32) Lee, J.-S.; Kim, S. T.; Cao, R.; Choi, N.-S.; Liu, M.; Lee, K. T.; Cho, J. *Adv. Energy Mater.* **2011**, *1*, 34.